Progress In Electromagnetics Research, Vol. 134, 111–131, 2013

LINK BUDGET OF MAGNETIC ANTENNAS FOR INGESTIBLE CAPSULE AT 40 MHz

F. El Hatmi*, M. Grzeskowiak, S. Protat, and O. Picon

Université Paris-Est, ESYCOM, Marne-la-Vallée, Cité Descartes, Marne-la-Vallée 77 454, France

Abstract—Magnetic antennas are suitable in short range medical in-body applications because they are less perturbed in the presence of the human tissues comparing to electrical antennas. After a preliminary study on magnetic antennas designed separately at 40 MHz with a matching system, a link budget between a spiral coil ingestible capsule transmitter antenna and a square coil on-body receiver antenna has been established in the presence of the human body. The efficiency (ratio of received power to transmitted power) of the magnetic induction link through a homogeneous human body (muscle) is equal to 0.6% when the TX (transmitter) capsule is in front of the RX (receiver) antenna. If the transmission channel is a three-layered human body (muscle/fat/skin) the performances of the inductive link can be enhanced and the efficiency reaches 0.8%. These performances can be improved (up to 1%) when the dimensions of the receiver antenna increase. Consequently, the power consumption can be reduced and hence the battery life of the wireless capsule increases. Additionally, when the TX antenna is located randomly at an arbitrary orientation and position, the efficiency of the magnetic induction link can be improved by orienting the RX antenna parallel and perpendicularly to the human body surface.

1. INTRODUCTION

The miniaturization of electronic components and antennas has permitted their use in a wide range of areas among which mobile phones, RFID tags and medical applications including pacemakers, retinal prosthesis, ingestible capsules, etc. The no invasive capsule systems are employed in the diagnosis and the monitoring of different

Received 12 August 2012, Accepted 15 October 2012, Scheduled 24 November 2012

* Corresponding author: El Hatmi Fatiha (elhatmi@univ-mlv.fr).

vital physiological parameters of the Gastro-Intestinal (GI) tract such as temperature, PH, pressure, and oxygen concentration [1–4]. Recently, endoscopy capsules were developed to send real-time GI tract images to an exterior base at high data rate which requires wideband antennas [5, 6]. In the design of the wireless ingestible capsule antenna, the size of the capsule, whose diameter is at most equal to 10.1 mm, needs to be considered [7]. In [4], ingestible capsules operating at VHF (32 and 40 MHz) and at UHF (868 MHz) are studied and it is shown that the capsules operating at the VHF presents generally better performances compared to UHF capsules. Also, an inductive link is carried out in [8] to wireless powering an implantable microwave by an external inductor. The implantable systems are not moving inside the human body contrarily to the ingestible devices.

The near field magnetic power, falls off as the inverse sixth power of distance in the near field [9] for ranges smaller than the wavelength while, in far field, the EM wave power decreases only with the inverse square of the distance, so magnetic antennas are generally not considered in the RF propagation systems which need to minimize the path losses in the transmission channel. However, this sort of antennas can benefit from the no-disturbance of the near field magnetic power in electrical lossy media. The opposite phenomenon is observed in dissipative media for the RF propagation, which suffers from high power absorption by the lossy media like human tissues and leads to low antenna's radiation efficiency in the human body which hardly exceeds 0.3% [10, 11].

In this paper, to assure an optimum signal transfer between the capsule antenna and the receiver antenna placed respectively inside and outside the human body, in-body and on-body small magnetic coil antennas operating at 40 MHz are first designed. Then, the efficiency of the near field magnetic induction link through the homogeneous human body, at different TX antenna positions and orientations, is estimated in order to realize an effective inductive link. Also, the H-field mappings are plotted for some inductive link configurations to illustrate the magnetic coupling between the TX and RX coil antennas. After that, a three-layered human body is used as a transmission channel to evaluate the influence of every human tissue layer in the performances of the magnetic induction link.

2. IN-BODY AND ON-BODY ANTENNAS DESIGN

The design of the antennas and the inductive link modeling in the presence of the human body was carried out using HFSS (High Frequency Structural Simulator) which is a commercial full wave

software based on the Finite Element Method (FEM) techniques. The in-body transmitter capsule antenna consists of a 10.1 mm diameter, 6-turn spiral coil spaced by a distance of 0.25 mm while the line width is equal to 0.2 mm as it is depicted by Fig. 1(a). It is inserted into a cylinder having the size of a capsule (vitamin pill) filled with air. A $10 \times 10 \times 10\,\text{cm}^3$ cubic box, having a permittivity ε_r of 83 and a conductivity σ of 0.67 S/m calculated thanks to the 4 cole-cole method [12] and representing a layer of average human muscles at 40 MHz, is used to simulate the TX antenna and the receiver coil presented in Fig. 1(c) and also to characterize the transmission channel illustrated by Fig. 1(b).

The on-body coil consists of a 4.1 cm × 4.1 cm, 4-turn squared spiral (Fig. 1(c)) whose both line width and spacing between turns are set to 0.3 mm. The on-body receiver coil is placed at about 5.2 cm from the TX coil. The Rogers RT/duroid 5880 substrate of thickness $h = 1.5$ mm, $\varepsilon_r = 2.2$ and dielectric loss tangent = 0.0009 is used to design both in-body and the on-body antennas.

3. INDUCTIVE LINK BUDGET THROUGH THE HOMOGENOUS HUMAN BODY

3.1. DIRECT H LINK (HL)

In this paragraph, we suppose that the transmitter capsule antenna is in front of the receiver antenna and the centers of both antennas are

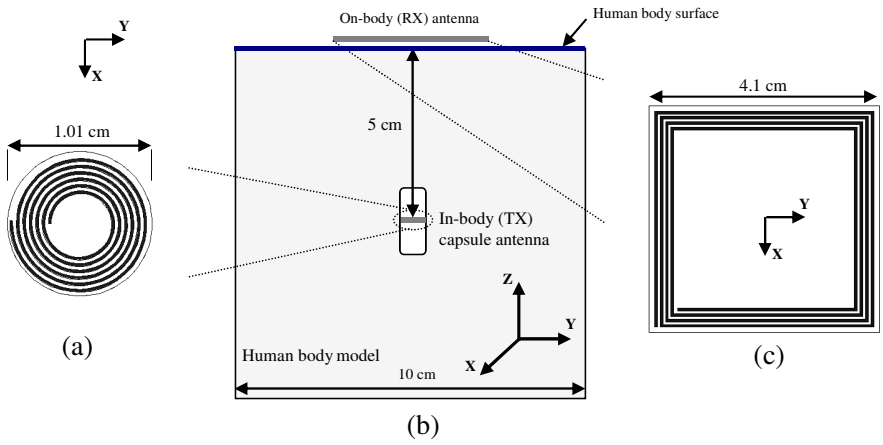

Figure 1. (a) Spiral coil TX antenna geometry (antenna 1); (b) Magnetic induction link through the homogeneous human body; (c) Square coil RX antenna geometry (antenna 2).

positioned at the origin of the OY axis. The surfaces of TX and RX antennas are parallel to the XOY plane. We note this transmission channel by direct H Link (HL): the RX antenna plane is parallel to the human body surface as it is presented in Fig. 1(b), the path loss is minimum because the path is perpendicular to the antenna's planes and the TX coil is in front of the RX antenna. This positioning suggests that the inductive link efficiency is optimum.

A matching system, composed of two capacitors and one parallel resistor, is designed for every antenna to adapt the antenna impedances close to 50 Ω. Each antenna is adapted alone, because the variation of the resonant frequencies of the magnetic antennas is negligible when the TX and RX antennas are used together. The −10 dB matching bandwidth is equal to 0.8% (around 0.33 MHz) for both in-body and on-body coils.

We performed two near field magnetic induction link budgets, one is through the homogeneous human body and the other is in the air, to evaluate the influence of the transmission channel in the performances of the inductive link.

Because the TX antenna is surrounded by the air volume of the capsule when it is inserted into the human body, the matching frequency of the transmitter antenna is not shifted when the transmission channel is the air as it is depicted by Fig. 2. However, we can see from Fig. 3 that the matching frequency of the RX antenna increases slightly in the air.

The magnetic field strength, narrated by mathematical expression (1) mainly depends upon the current (I), the loop radius (R), the

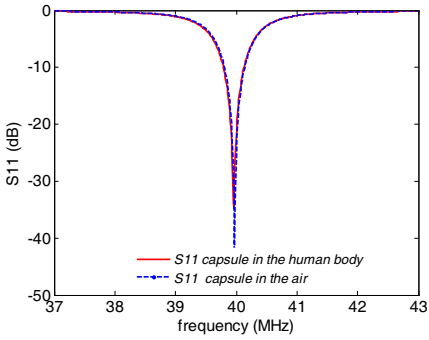

Figure 2. Simulated return loss of the TX antenna in the human body and in the air.

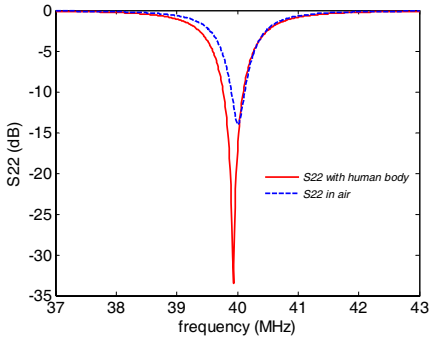

Figure 3. Simulated return loss of the RX antenna when the transmission channel is the human body and the air.

number of the loop turns (N) and the distance from the center of the coil in the normal z-direction [13].

$$H = \frac{I \times N \times R^2}{2 \times \sqrt{(R^2 + z^2)^3}} \tag{1}$$

If we consider a magnetic induction link between transmitting and receiving coils in near field, the received power P_R, expressed by the following relation (2) at the operating frequency, depends on the quality factors (Q_T and Q_R), the efficiencies (η_T and η_R), the radii (r_T and r_R) of the transmitter and the receiver coils, the transmission power (P_T) and the distance between the transmitter and the receiver (d) and can be expressed as follows [14]:

$$\begin{aligned} P_R(\omega) &= P_T \times \eta_T \times \eta_R \times Q_T \times Q_R \times k^2(d) \\ &= P_T \times \eta_T \times \eta_R \times Q_T \times Q_R \times \frac{r_T^3 \times r_R^3 \times \pi^2}{(r_T^2 + d^2)^3} \end{aligned} \tag{2}$$

where (k) represents the coupling coefficient between the two coils.

At 40 MHz, the wavelength in free space is 750 cm and due to the high permittivity of the media, value reduces to 53 cm [12] if the transmission channel is the muscle. Taking into account the classic near field zone limit of $\lambda/2\pi$, the distance of 8.5 cm seems to be a limit of the near field inductive coupling between the TX and RX coil antennas in the muscle. As the depth of the small intestine from the human body surface (interface skin-air) is considered generally to be equal to 5 cm [10], we have supposed that the distance between the in-body and the on-body antennas in the z direction is equal 5.2 cm to report the link budget (S_{21}) where 0.2 cm corresponds to the minimum air gap between the RX antenna and the body surface, because the receiver antenna must be enough away from the body phantom to operate correctly as an inductive circuit.

In order to estimate the power level received by the RX coil, a near field magnetic induction link budget has been carried out. The S_{21} parameter (efficiency), that characterizes the inductive link, is equal to the ratio of received power to transmitted power. According to (2), the S_{21} response can be expressed by (3), where η_T, η_R, Q_T, Q_R and k [9] are:

$$S_{21} = \frac{P_L}{P_S} = \eta_T \eta_R Q_T Q_R k^2(d) \tag{3}$$

$$\eta_T = \frac{R_S}{R_S + R_{LT}}; \quad \eta_R = \frac{R_L}{R_L + R_{LR}} \tag{4}$$

$$Q_T = \frac{\omega_0 L_T}{R_S + R_{LT}}; \quad Q_R = \frac{\omega_0 L_R}{R_L + R_{LR}} \tag{5}$$

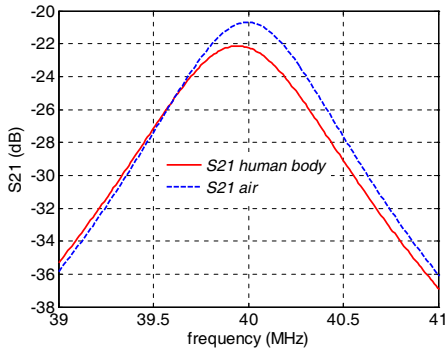

Figure 4. Simulated transmission parameter in free space and in the presence of the human body.

$$k = \frac{M}{\sqrt{L_T L_R}} \tag{6}$$

R_{LT} and R_{LR} are the resistances of the transmitter and the receiver coils respectively. R_S and R_L are the source and the load resistances respectively. L_T and L_R are the inductances of the transmitter and the receiver coils respectively and M is the mutual inductance.

Figure 4 reports the simulated S_{21} parameter in free space and in the presence of the human body. The S_{21} response is slightly modified by the body presence. It decreases from -20.7 dB in the air to -22.1 dB in the human body at around 40 MHz. Moreover, the efficiency, represented by the S_{21} parameter, is found to be equal to 0.6% (-22.1 dB) in the human body. The radiation efficiencies of the electromagnetic links through the human body are narrated in the literature for two different frequencies; at 1.4 GHz, when a meandered antenna is conformed on the capsule in the small intestine, the efficiency is equal 0.1% [10], while at 402 MHz, it is equal 0.3% for an implanted spiral PIFA antenna [11]. Furthermore, the radiation efficiency is found to be less than 0.1% at 404.5 MHz and can achieve 0.9% at 2.387 GHz for a multilayered spiral implanted antenna when the body phantom is a 3-layered cylindrical model [15].

We also calculated, from the scattering parameters of the RX and TX antennas, the coupling coefficient k around 40 MHz (6) in free space and in the presence of the human body. We found that k, which is generally comprised between 0 and 1, is equal to 0.05 in free space and 0.04 in the human body. These low values are essentially due to the small dimensions of the coil antennas, particularly the transmitter capsule antenna. Then, we calculated the theoretical S_{21} parameter narrated by (3) in each media at 40 MHz after calculating η_T, η_R,

Table 1. Theoretical calculation of the antenna characteristics and the S_{21} parameter in the presence of the human body and in free space at 40 MHz.

		Human body	Free space
R_{LT} (Ω)		0.8	0.8
R_{LR} (Ω)		7	4
X_T (Ω)		74.5	74.5
L_T (μH)		0.3	0.3
X_R (Ω)		514	512
L_R (μH)		2	2
Q_T		1.5	1.5
Q_R		9	9.5
η_T		0.98	0.98
η_R		0.88	0.92
k		0.04	0.05
S_{21}(dB)	theoretical	-17.3	-15
	simulation	-22.1	-20.7
ΔS_{21} (dB)		4.8	5.7
S_{21}(%)	theoretical	1.8	3.1
	simulation	0.6	0.85
ΔS_{21} (%)		1.2	2.25

$\Delta S_{21} = S_{21(\text{theoretical})} - S_{21(\text{simulation})}$.

Q_T and Q_R from (4) and (5). The resistances R_S and R_L are set to 50 Ω and P_T is set to 1 W while R_{LT}, R_{LR}, L_T, and L_R are deducted from the simulated parameters of the TX and RX antenna. All these parameters and the results are given by Table 1.

We can conclude from Table 1 that the modification of the media affects the input impedance of the receiver coil and so the link budget. However the parameters of the transmitter coil (R_{LT} and L_T) do not vary when the media change from the human body to the air and then Q_T and η_T do not also vary. This is due to the presence of the capsule filled with air, in which the in-body antenna is inserted. Also, the theoretical results obtained show a good agreement with simulated results. So, the difference between the theoretical and the simulated results $\Delta S_{21}(\%) = S_{21(\text{theoretical})}(\%) - S_{21(\text{simulation})}(\%)$ is 1.2% in the human body and 2.25% in the air when $S_{21}(\%) = 0.01 * 10^{(S21(\text{dB})/10)}$.

Additionally, through HFSS simulation, we estimated the value of the magnetic flux through some surfaces parallel to the XOY plane at different z-positions in the presence of the RX antenna. The OZ axis

is normal to each surface at its origin. The magnetic flux is equal to: $\Phi = B \cdot S$, when S is the surface in m^2 and B is the magnetic induction in Tesla. Then, we have estimated the reactive power density given by $P = \omega |B|^2 / 2\mu_0$ at different surfaces. Table 2 summarizes the obtained results when the transmitted power is set to 1 W and shows that the power density falls off with a factor of 10^{-6} if the z-distance increases from 1 cm to 5.35 cm and attains $5.5 \times 10^{-5}\,\mathrm{W \cdot m^{-2}}$ at the plane of the RX coil.

We can also see the H-field lines at 40 MHz in the human body through the mapping illustrated by Fig. 5 which shows that the field lines are perpendicular to the RX antenna surface. So, the transmission channel is in its optimum configuration.

The capsule antenna presents a size limitation, while less restrictions concern the RX antenna which is located on the body surface. We have modified the sizes of the receiver coil to 5 cm × 8 cm, the turn number, line width and gap between the lines are set to 3, 2 mm and 2 mm respectively and we have determined the new values of the matching system components according to the input impedance of the receiver antenna. Consequently, the efficiency of the inductive link is improved and reaches 1% while the quality factor is equal to 4.8.

In the rest of the paper, we select the receiver coil defined in the

Table 2. Power density at different planes from the TX antenna.

Distance [oz]	**1 cm**	**2 cm**	**3 cm**	**4 cm**	**5 cm**	**5.35 cm**
P $(\mathbf{W \cdot m^{-2}})$	84.17	2.5	2.2×10^{-1}	3×10^{-2}	1.1×10^{-3}	5.5×10^{-5}

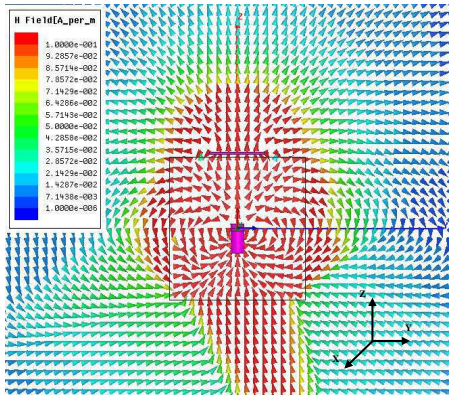

Figure 5. H-field lines through the human body in the direct HL at 40 MHz.

beginning (4.1 cm × 4.1 cm) while the z distance between the TX and RX antennas is kept constant and equal to 5.2 cm. We have chosen this on-body antenna because it presents an acceptable transmission parameter (−22.1 dB) with a moderate size (the overall surface is less than 17 cm^2).

As the capsule antenna slides down into the gastrointestinal tract randomly, it is necessary to analyze the influence of the variation of the TX antenna position and orientation in the inductive link efficiency to evaluate the performances of the transmission channel.

3.2. TX ANTENNA ANGLE VARIATION

Taking into account the fact that the TX capsule antenna orientation can easily change when the capsule moves through the gastrointestinal-tract, a series of simulation have been carried out.

3.2.1. Angle Variation in the H Link (HL)

In the H Link (HL), the RX antenna is parallel to the surface of the human body which is according to the XOY plane. We report in Fig. 7, the evolution of the transmission parameter versus the frequency when the TX antenna orientation is from 0° to 90° in the YOZ plane as it is shown in Fig. 6. It is clear from Fig. 7 that the efficiency of the inductive link has greatly deteriorated above the angle of 70°. If we consider that the acceptable efficiency level limit is equal to −32 dB (0.06%) at 40 MHz, the orientation of the in-body antenna from 70° to 90° does not satisfy the data transmission conditions. So,

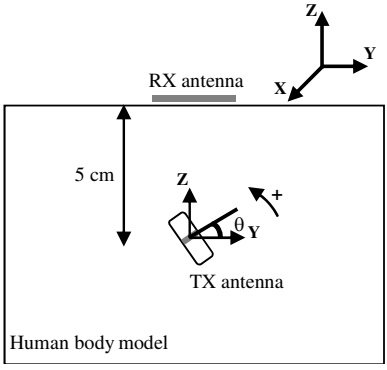

Figure 6. TX antenna angle variation in the HL.

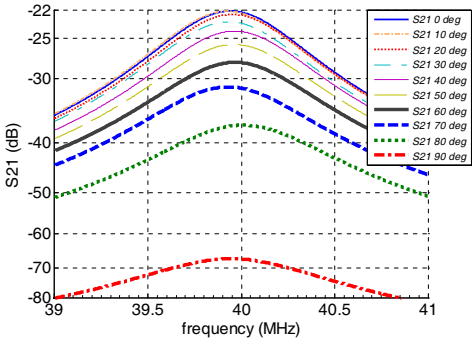

Figure 7. Simulated S_{21} parameter according to the frequency when θ varies from 0° to 90° in the HL.

a complementary study where the RX antenna is oriented in the XOZ plane and perpendicularly to the human body surface may solve this problem. We note this second channel by V Link (VL) because the receiver antenna is perpendicular to the human body surface.

3.2.2. Angle Variation in the VL

In the VL, the orientation of the TX antenna is identical to that of the HL; the only difference between the two scenarios concerns the relative orientation of the RX antenna which is perpendicular to the body surface in the VL. Fig. 8(a) shows the VL channel configuration in the optimum case while Fig. 8(b) illustrates how the orientation of the TX antenna can change from 90° to 0°. According to Fig. 9, the transmission parameter at 40 MHz is around −32 dB if θ varies between 90° and 70°. This can solve the problem concerning the weak level of the S_{21} parameter in the HL and thus the combination of HL and VL can cover all TX antenna orientations. When the angle θ is below 60°, the VL link is no longer effective.

3.2.3. Angle Variation in the HL and the VL

Figure 10 shows the variation of the transmission parameter according to the angle θ around 40 MHz in both cases of HL and VL defined above. We can see from these plots that the HL and the VL are complementary. In other words, if the HL performances decrease (when θ is between 70° and 90°), the VL link becomes efficient and vice versa. So, by the combination of the HL and the VL, the channel efficiency is always better than −32 dB for all TX antenna orientations when

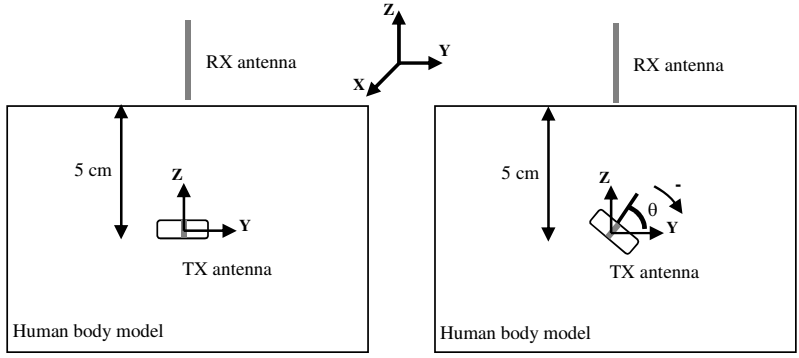

Figure 8. (a) RX antenna orientation in the VL; (b) TX antenna angle variation in the VL.

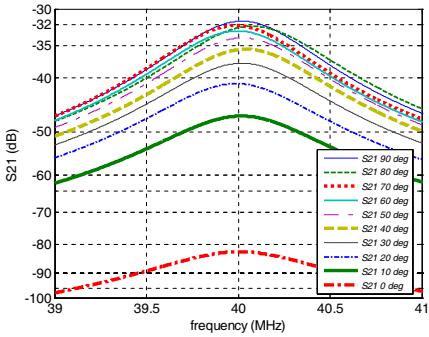

Figure 9. Simulated S_{21} parameter according to the frequency when θ varies from 90° to 0° in the VL.

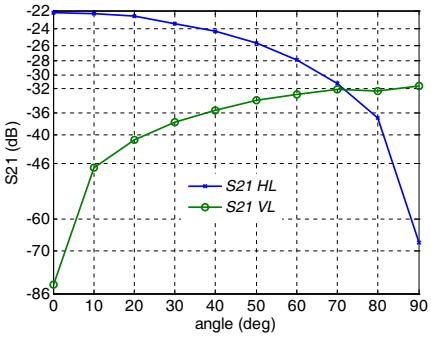

Figure 10. Simulated transmission parameter according to the angle θ at 40 MHz in the HL and the VL.

the capsule antenna position does not change with regard to that of the RX antenna. It is also clear from Fig. 10 that the VL is found to yield poor performances compared to the HL essentially because the upper limit of the S_{21} parameter (−32 dB) occuring at $\theta = 90°$ in the VL is lower than the highest transmission parameter level found in the case of the HL (−22 dB). The RX antenna perpendicular to the human body surface can be improved to be less cumbersome.

To conclude, we have to set a combination of perpendicular and parallel segments of RX antennas, taking into account the coupling between them, to offer optimum inductive link with a maximum power transfer. So, we have performed the transmission channel when two RX antennas are simultaneously positioned parallel and perpendicularly to the human body surface in order to study the coupling between the two RX antennas and to evaluate the channel efficiency. This configuration, noted by RX antenna network link, is illustrated by Fig. 11 and the inductive link efficiency at 40 MHz according to the orientation of the TX antenna is depicted by Fig. 12. So, the S_{21} parameter corresponds to the transmission parameter between the capsule antenna and the perpendicular RX antenna while the S_{31} parameter is related to the transmission parameter between the TX antenna and the parallel RX antenna. We can conclude that the plots of Fig. 12 are close to these of Fig. 10 when the HL and the VL were taken separately. Therefore, we can say that the coupling effect between the two RX antennas does not affect the channel efficiency in the case of RX antenna network link: a low masking effect can be seen by a slight modification of the S_{21} parameter in the intersection of both curves from −32 dB (Fig. 10) to −33 dB (Fig. 12).

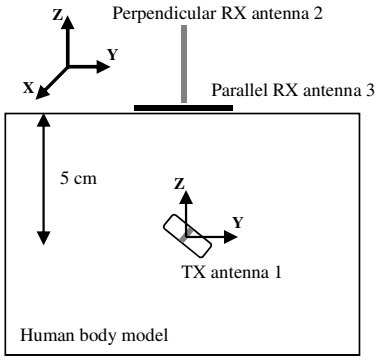

Figure 11. Structure of the RX antenna network link through the human body.

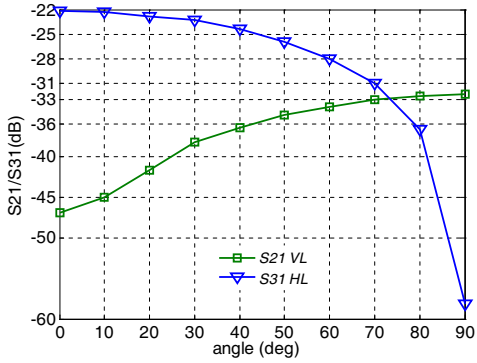

Figure 12. Simulated transmission parameter according to the angle θ at 40 MHz in the RX antenna network link.

3.3. TX Antenna Position Variation

The position of the in-body antenna can also vary with reference to that of the receiver antenna. Therefore, it is imperative to study the TX antenna position variation according to the OY axis which is illustrated by Fig. 13 and Fig. 14 for the HL and the VL respectively. In this paragraph, only the position of the TX antenna varies, its orientation is considered optimal for each channel configuration. So, the angle θ that defines the orientation of the capsule antenna is equal to 0° in the HL and to 90° in the case of the VL. Furthermore, we consider that the position of the transmitter coil according to the OY axis corresponds approximately to the spacing between the center of the capsule antenna and that of the RX antenna in the y direction.

The plots of Fig. 15 show the variation of the S_{21} parameter according to the distance in both HL and VL at 40 MHz.

It is clear from Fig. 15 that the S_{21} parameter related to the HL decreases when the TX antenna retards away from the RX antenna while the HL efficiency remains suitable even at $y = \pm 3$ cm which presents the lowest S_{21} value (−28 dB). Concerning the VL, the S_{21} value drops from −32 dB for $y = 0$ cm to −40 dB when $y = \pm 3$ cm. However, until $y = \pm 1$ cm, the S_{21} value is still close to −32 dB.

Furthermore, having considered only the TX antenna position variation, the efficiency of the HL is better than that of the VL regardless of the position of the TX antenna, when the distance is −3 cm and 3 cm in y direction. Additionally, we can also conclude from Fig. 15 that the gap between the S_{21} parameter in the HL and

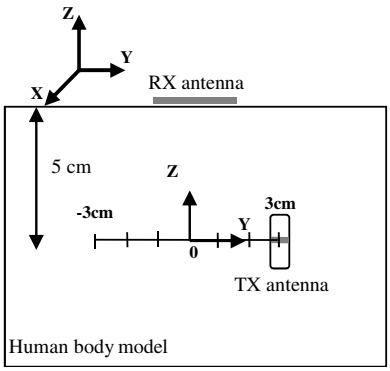

Figure 13. TX antenna position variation according to the *OY* axis in the HL.

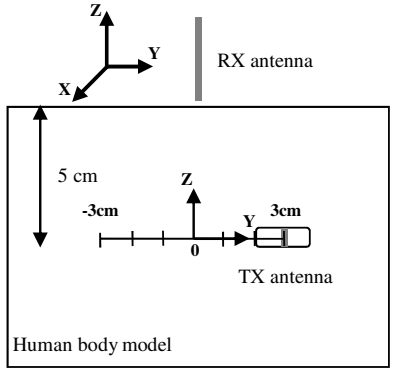

Figure 14. TX antenna position variation according to the *OY* axis in the VL.

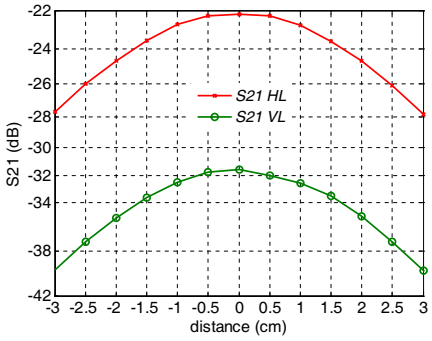

Figure 15. Simulated transmission parameter according to the distance at 40 MHz in the HL and the VL.

the VL is almost equal to −10 dB (±2 dB) at every capsule antenna position.

This study has allowed estimating the performances of the transmission channel when only the distance between the TX and the RX antennas varies, but it has to be completed by a study of the channel efficiency when the orientation and the position of the capsule antenna change together.

3.4. TX Antenna Angle and Position Variation

The ingestible capsule antenna may be positioned randomly when it slides down into the gastro-intestinal tract, in other words, the position

and the orientation of the in-body antenna can vary together. So, we have performed separately the transmission channel of the HL and the VL by varying both the position and the angle of the in-body antenna. The evolution of the S_{21} parameter according to the angle in different y-position sat 40 MHz is depicted by Fig. 16 divided in four parts, where every portion corresponds to a TX antenna y-position ($y = 0$, -1, -2 and -3 cm). We can conclude from these plots that for all selected y-positions, the HL and the VL are complementary. Moreover, we can say that the evolution of the transmission parameter versus the transmitter antenna orientation in the HL and the VL depends on the relative y-position. As depicted in Fig. 16, when the relative distances between the two antennas are $y = -1$ cm, -2 cm and -3 cm, the S_{21} value decreases as θ increases in the beginning and then it increases after the θ value reaches 80°, 60° and 50° for each relative position respectively. In fact, when the in-body capsule moves away from the RX antenna, the H-field lines received by the on-body antenna can be optimized by the rotation of the TX antenna. Additionally, when the level of the S_{21} parameter in the HL becomes low for some transmitter coil orientations, the corresponding S_{21} for the VL can give acceptable inductive link efficiency.

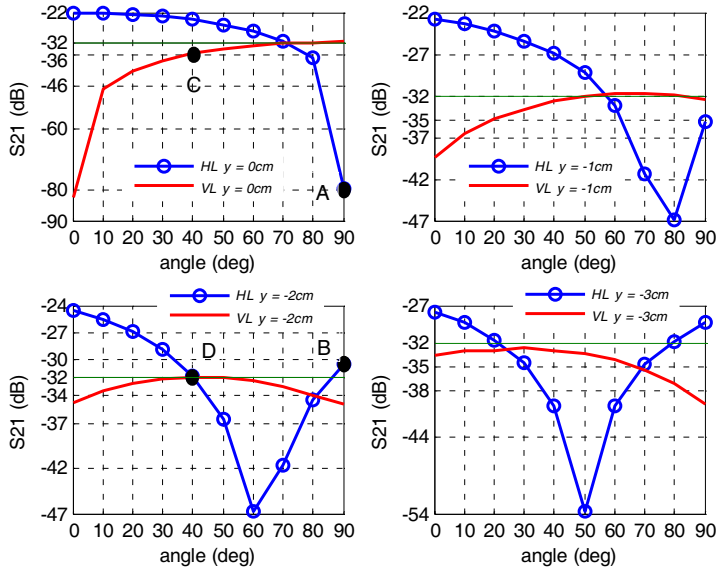

Figure 16. Simulated transmission parameter at different TX antenna y-positions as a function as the angle θ at 40 MHz in the HL and the VL.

To conclude, we should set an array of perpendicular and parallel segments of RX antennas, taking into account the on-body antenna sizes as well as the space and the coupling between them, to offer optimum inductive link with a maximum power transfer. We remember that the y-position corresponds to the spacing between the centers of the in-body and the on-body antennas in the y direction. So, the previous study allows to fix the maximum shift between the TX and the RX antenna centers which is estimated to be equal to 2 cm according to the results of Fig. 16: the S_{21} value always stands between -22 dB and -32 dB (it is equal to -34 dB only at $y = -2$ cm when θ is around 80°). The RX antenna size, initially equal to 4.1 cm × 4.1 cm can be reduced to 4 cm × 4 cm. Therefore, to get an effective inductive link, the proposed RX antenna array will be constituted by adjacent sections of parallel RX antennas and segments of perpendicular RX antennas spaced by 4 cm. The study concerning the variation of the transmitter antenna position according to the OX axis is similar to this one in the y-direction. To avoid encumbering this network by the RX square coil antennas oriented perpendicularly to the surface of the human body, we envisage replacing the perpendicular RX antenna by solenoids of smaller sizes which can be more easily mounted in the RX antenna array.

To better display these phenomena, the H-field lines are reported in Fig. 17 and Fig. 18 for some of the previously defined cases. We can see the mapping of the H-field lines in the HL at 40 MHz when θ is equal to 90° and the transmitter coil y-position is equal to 0 cm and -2 cm respectively in Fig. 17(a) and Fig. 17(b). In this channel configuration, if $y = 0$ cm, the H-field lines are adjacent to the RX antenna surface and this can explain why the S_{21} parameter is very low in this case ($S_{21} = -79.6$ dB: point A of Fig. 16). When the distance between the TX and the RX antennas is 2 cm, there is some H-field lines which can be perpendicular to the RX antenna surface that leads to seriously improve the inductive link efficiency ($S_{21} = -31.5$ dB: point B of Fig. 16).

In the same manner, the H-field lines topology in the VL at 40 MHz when θ is equal to 40° and the transmitter coil y-position is equal to 0 cm and -2 cm are depicted respectively in Fig. 18(a) and Fig. 18(b). In this channel configuration, when the TX antenna is in the center of the OY axis, the H-field lines going through the surface of the RX antenna are not totally perpendicular to the receiver coil. This leads to a weak level of the S_{21} parameter (-36 dB: point C in Fig. 16). If $y = -2$ cm, the H-field lines are almost perpendicular to the RX antenna surface and consequently the S_{21} response is better ($S_{21} = -32$ dB: point D in Fig. 16).

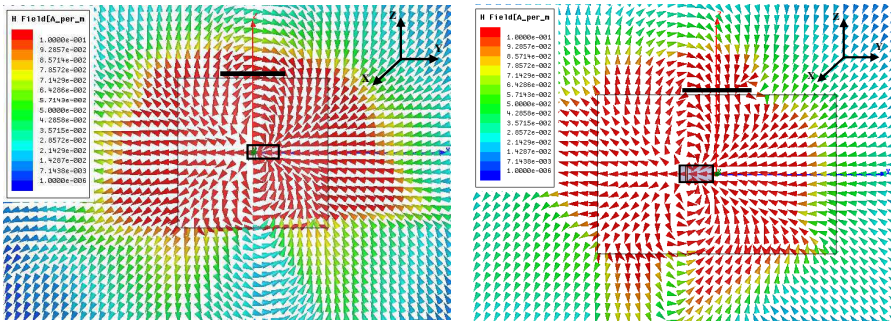

Figure 17. H-field lines in the HL at 40 MHz when θ is equal to 90°: (a) The y-position is equal to 0 cm; (b) The y-position is equal to −2 cm.

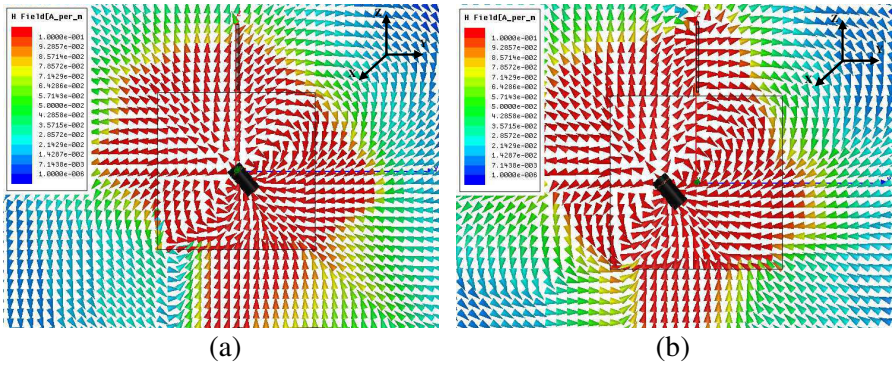

Figure 18. H-field lines in the VL at 40 MHz when θ is equal to 40°: (a) The y-position is equal to 0 cm; (b) The y-position is equal to −2 cm.

4. INDUCTIVE LINK BUDGET THROUGH A TREE-LAYERED HUMAN BODY

In this section, we have used a three-layered human body model which is more realistic than the homogeneous model and this study concerns only the direct HL with its optimum configuration ($y = 0$ cm and $\theta = 0°$). So, fat and skin layers cover the muscle while keeping the distance between the TX and RX antennas constant (5.2 cm).

First, we consider a layer of muscle whose thickness is equal to 3.5 cm covered by 1.4 cm of fat which is also covered by 1 mm of skin as illustrated in Fig. 19. These values are chosen randomly: the thickness of each body tissue varies with the person.

Each kind of human tissue is characterized by its own dielectric properties, which depends on the frequency. The electrical characteristics of the three tissues used in the proposed human body model at 40 MHz can be found in Table 3.

Figure 20 shows the evolution of the transmission parameter as a function of the frequency when the transmission channel is the air, the homogeneous human body and the three-layered human body. It is clear from these plots that the inductive link efficiency can be improved when the human body is composed of three layers and gets close to the efficiency of the link through the air. Table 4 summarizes these results at the operating frequency: the S_{21} parameter can be improved by 1 dB when the muscle is covered by fat and skin layers compared to the homogeneous human body.

So, the dissipated energy in the lossy medium is converted to heat and the losses are proportional to the volume and the conductivity of each kind of body tissue [16]. Therefore, we can explain these results

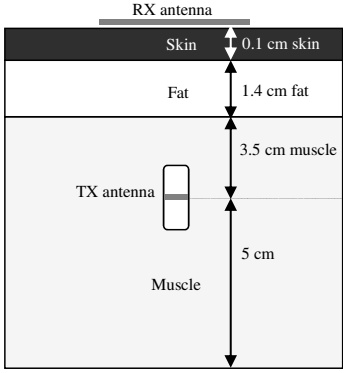

Figure 19. Magnetic induction link through a three-layered human body (muscle/fat/skin).

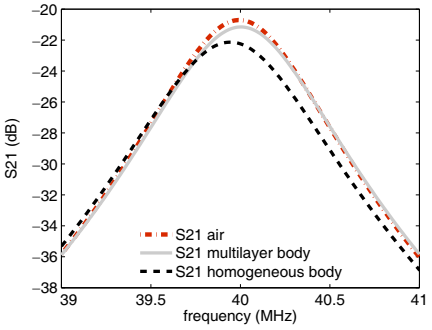

Figure 20. Simulated S_{21} parameter as a function of the frequency in the three-layered human body.

Table 3. Dielectric properties of human tissues employed in the three-layered human body at 40 MHz.

Human tissue	Relative permittivity	Conductivity (S/m)
Muscle	82.6	0.67
Fat	7.3	0.034
Skin	124.3	0.38

Table 4. Simulated S_{21} parameter of the inductive links through the air, the three-layered human body and the homogeneous model at 40 MHz.

	Air	Three-layered model	Homogeneous model
S_{21} (dB)	−20.7	−21.1	−22.1

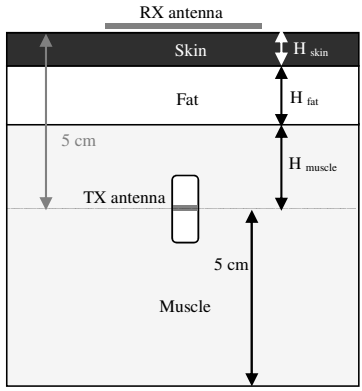

Figure 21. Inductive link through a three-layered human body: parametric study as a function as the thickness of body tissues.

by the very low conductivity of the fat at 40 MHz (0.034 S/m) which is close to that of the air (0 S/m) while the conductivity of the muscle is equal to 0.67 S/m.

It is also necessary to study the influence of the thickness of different tissues on the transmission channel performances. In the following paragraph, a parametric study, regarding the tissue thickness, has been carried out when the transmission channel is a three-layered human body. The distance between the TX and RX antennas is kept constant and equal to 5.2 cm (5 cm of muscle, fat and skin and 0.2 cm of air) as it is shown in Fig. 21.

At the beginning, we kept the skin thickness (H_{skin}) constant and equal to 1 mm and we varied only the fat thickness (H_{fat}) from 2 mm to 20 mm. We assume that the distance between the TX and RX antennas is constant, to estimate the modification due to the fat layer, therefore the muscle thickness (H_{muscle}) depends on the thickness of fat ($H_{\text{muscle}} = 4.9\,\text{cm} - H_{\text{fat}}$). The results are depicted in Fig. 22 and show that the efficiency of the inductive link increases by almost 0.7 dB, from −21.7 dB to −21 dB, when H_{fat} rises from 2 to 20 mm.

Then, we varied the skin thickness (H_{skin}) from 1 mm to 5 mm at two scenarios: when H_{fat} is equal to 1.4 cm and to 2 cm. The muscle

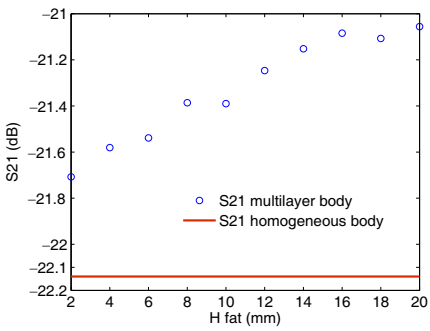

Figure 22. Simulated transmission parameter in the three-layered human body as a function of H_{fat} at 40 MHz.

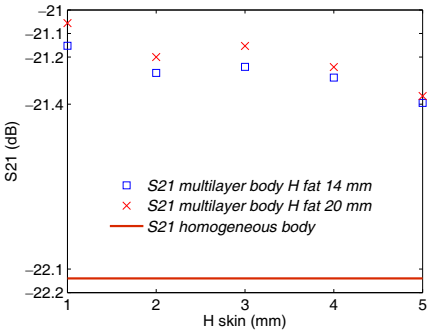

Figure 23. Simulated transmission parameter in the three-layered human body as a function of H_{skin} at 40 MHz.

thickness in this case is equal to: $H_{\text{muscle}} = 5\,\text{cm} - H_{\text{fat}} - H_{\text{skin}}$. Contrarly to the previous case, the efficiency of the inductive link decreases slightly, when H_{skin} rises from 1 mm to 5 mm: it drops from almost -21.1 dB to -21.4 dB and from approximately -21 dB to -21.4 dB if H_{fat} is equal to 1.4 cm and to 2 cm respectively as it is shown by Fig. 23. This can be explained by the high conductivity of skin that is equal to 0.38 S/m at 40 MHz while the conductivity of fat is only equal to 0.034 S/m. So, the results can be enhanced by increasing the fat layer thickness. Although the inductive link efficiency drops off when H_{skin} increases, the S_{21} parameter stays better than that found in the homogeneous human body channel, which is equal to -22.1 dB thanks to the presence of the fat layer.

We can conclude that when the distance between the TX and RX antennas is kept constant, the fat layer allows to improve significantly the performances of the inductive link whereas the influence of the skin layer is not very prominent.

5. CONCLUSION

Magnetic antennas, generating H-field in the near field region which is independent of the variation of the dielectric properties of the transmission channel, have been investigated to establish an efficient inductive link between antennas placed inside (TX antenna) and outside (RX antenna) the human body. The efficiency of this inductive link obtained when the TX antenna is directly in front of the RX antenna is equal to 0.6% and can be improved if the dimensions of the RX antenna increase. The fat layer can also enhance the performances

of the inductive link by 0.2% because of its low conductivity at 40 MHz. Consequently, a more realistic multi-layered human body allows promoting the signal transfer between the in-body capsule antenna and the on-body receiver antenna.

The capsule antenna is located anywhere at any orientation in the gastro-intestinal tract, in order to overcome this problem and to guarantee an adequate power transfer, RX on-body antennas have been positioned parallel and perpendicularly to the human body surface. Hence, we have defined two channel configurations: a HL and a VL studied independently according to the TX antenna orientation and position. Then, an array combining perpendicular and parallel RX antennas has been proposed. The results showed that, regardless of the orientation and the position of the capsule antenna in the gastro-intestinal tract, the magnetic induction link remains efficient.

Furthermore, to promise a higher power transfer through the human body and to maximize the efficiency of the inductive link beyond 1%, we propose to increase the dimensions of the RX antenna while the size of the TX antenna is limited by the capsule dimensions. It will be the future work of this study that includes also the realization of antennas and the measurements of different antennas characteristics as well as the link budget.

REFERENCES

1. Yan, G., B. Huang, and P. Zan, "Design of battery-less and real-time telemetry system for gastrointestinal applications," *IEEE International Conference on Control and Automation*, 245–249, May 30–Jun. 1, 2007.
2. Aydin, N., T. Arslan, and D. R. S. Cumming, "Design and implementation of a spread spectrum based communication system for an ingestible capsule," *Biomedical Engineering Society EMBS/BMES Conference*, Vol. 2, 1773–1774, 2002.
3. Kim, Y., et al., "Pressure monitoring system in gastro-intestinal tract," *Proceedings of the IEEE International Conference on Robotics and Automation*, 1321–1326, Apr. 18–22, 2005.
4. Wang, L., T. D. Drysdale, and D. R. S. Cumming, "In situ characterization of two wireless transmission schemes for ingestible capsules," *IEEE Transactions on Biomedical Engineering*, 2020–2027, Nov. 2007.
5. Zhao, D., X. Hou, X. Wang, and C. Peng, "Miniaturization design of the antenna for wireless capsule endoscope," *4th International Conference on Bioinformatics and Biomedical Engineering (iCBBE)*, 1–4, 2010.

6. Izdebski, P. M., H. Rajagopalan, and Y. Rahmat-Samii, "Conformal ingestible capsule antenna: A novel chandelier meandered design," *IEEE Transactions on Antennas and Propagation*, 900–909, Apr. 2009.
7. Kwak, S. I., K. Chang, and Y. J. Yoon, "Small spiral antenna for wideband capsule endoscope system," *Electronics Letters*, Vol. 42, 1328–1329, Nov. 9, 2006.
8. Tikka, A. C., M. Faulkner, and S. Al-Sarawi, "Secure wireless powering and interrogation of an implantable microvalve," *IEEE Topical Conference on Biomedical Wireless Technologies, Networks, and Sensing Systems (BioWireleSS)*, 35–38, Jan. 16–19, 2011.
9. Agbinya, J. I., et al., "Size and characteristics of the 'cone of silence' in near-field magnetic induction communications," *Journal of Battlefield Technology*, Vol. 13, No. 1, Mar. 2010.
10. Rajagopalan, H. and Y. Rahmat-Samii, "Link budget analysis and characterization for ingestible capsule antenna," *International Workshop on Antenna Technology (iWAT)*, 1–4, Mar. 1–3, 2010.
11. Yahya, R.-S. and K. Jaehoon, *Implanted Antennas in Medical Wireless Communications*, 1st Edition, Morgan & Claypool Publishers' Series, Ed., USA, 2006.
12. Dielectric Properties of Human Tissues [on line] available: niremf.ifac.cnr.it/docs/DIELECTRIC/AppendixC.html#FF.
13. Finkenzeller, K., *RFID Handbook: Radio-frequency Identification Fundamentals and Application.*, 2nd Edition, Wiley, 2003.
14. Agbinya, J. I. and M. Masihpour, "Near field magnetic induction communication link budget: Agbinya-Masihpour model," *Fifth International Conference on Broadband and Biomedical Communications (IB2Com)*, 1–6, 2010.
15. Merli, F., et al., "Design, realization and measurements of a miniature antenna for implantable wireless communication systems," *IEEE Transactions on Antennas and Propagation*, Vol. 59, No. 10, 3544–3555, Oct. 2011.
16. Hennig, A., "RF energy transmission for sensor transponders deeply implanted in human bodies," *38th Microwave Conference EuMC*, 424–427, 2008.